Journal of chemical & engineering data

Article

Cite This: J. Chem. Eng. Data XXXX, XXX, XXX−XXX

pubs.acs.org/jced

Liquid−Liquid Equilibrium and Extraction Performance of Aqueous Biphasic Systems Composed of Water, Cholinium Carboxylate Ionic Liquids and K_2CO_3

Mafalda R. Almeida,[†] Diana C. V. Belchior,[†] Pedro J. Carvalho,[†] and Mara G. Freire*,[†]

[†]CICECO—Aveiro Institute of Materials, Department of Chemistry, University of Aveiro, 3810-193 Aveiro, Portugal

Supporting Information

ABSTRACT: Ionic-liquid-based aqueous biphasic systems (IL-based ABS) have been broadly investigated for the separation of high-value compounds. Nevertheless, the large-scale application of IL-based ABS is still hampered by the high cost and hazardous features of most ILs used. Aiming at characterizing novel ABS composed of ILs with a more acceptable environmental footprint and enhanced biocompatibility, in this work, ABS formed by water, cholinium carboxylate ILs ([Ch][C_nCO_2], with n = 2 to 6), and K_2CO_3 were investigated. The respective ternary phase diagrams, including binodal curves, tie-lines, and critical points, were determined at (298 ± 1) K and atmospheric pressure. The capability to form ABS (or of the IL to be salted-out) increased with the increase of the alkyl chain length of the IL anion up to cholinium pentanoate; however, for longer anion alkyl chain lengths the ILs self-aggregation led to a decrease of the ILs ability to form ABS. Furthermore, the liquid−liquid equilibrium data experimentally determined were modeled using the local composition activity model NRTL (nonrandom two liquid). The extraction performance of these systems was finally evaluated with four nitrogenous bases (thymine, adenine, guanine, cytosine). In all studied systems nitrogenous bases preferentially migrated to the IL-rich phase, with extraction efficiencies ranging between 81% and 97% in a single-step. The determined novel phase diagrams indicate the composition of the mixtures required to use IL-based ABS as separation routes. The extraction performance evaluation of these systems with nitrogenous bases provides an indication of their possible application to isolate high-value compounds with biotechnological interest.

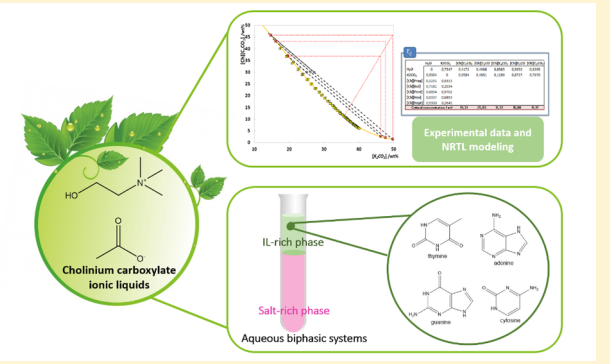

INTRODUCTION

Ionic-liquid-based aqueous biphasic systems (IL-based ABS) formed by ILs, inorganic salts, and water were proposed in 2003 by Gutowski et al.[1] as promising alternatives over more conventional ABS constituted by polymers.[2] They are usually less viscous than polymer-based systems and display faster phase separation rates, which is also promoted by a higher difference in the densities of the respective phases.[3−5] These advantages led to intensive research in the past 15 years on ILs as alternative phase-forming components of ABS.[6−10] In addition to their nonvolatility that has been seen as one of the more important features, the designer solvent ability of the ILs, which can be achieved by modifying either the cation or the anion chemical structure, is one of the most relevant properties when addressing their use in ABS and separation processes, although imidazolium-based ILs, most of the time combined with halogens and $[BF_4]^-$ as anions, are still the preferred choice.[11]

Large efforts have been placed in the past years to synthesize novel ILs with both an acceptable environmental footprint and enhanced biocompatibility.[12] Among these, ILs comprising the 2-hydroxyethyl-*N*,*N*,*N*-trimethylammonium (cholinium) cation stand out due to their high biodegradability and marginal toxicity if properly designed.[13,14] On the basis of these advantages, several works have described the use of cholinium-based ILs in the formation of ABS.[15−18] However, cholinium-based ILs tend to be highly hydrophilic and only form ABS with strong salting-out salts (e.g., K_3PO_4[11,13,19] and K_2CO_3[11]) or with polymers (e.g., polypropylene glycol (PPG) 400 and 1000,[16,17,20,21] polyethylene glycol (PEG) 400, 600 and 1000,[22] polyethylene glycol-*block*-polypropylene glycol-polyethylene glycol[21]), in which the IL may act as the salting-out species.

With this work we aim to expand the characterization of ABS formed by cholinium-based ILs and salts, demonstrating that novel ABS can be formed if combining cholinium carboxylate ILs and K_2CO_3 in aqueous media. The respective ternary phase diagrams, including binodal curves, tie-lines, and critical points, were determined at (298 ± 1) K and atmospheric pressure. To infer the possible application of

Special Issue: Celebrating Our High Impact Authors

Received: May 22, 2019
Accepted: October 3, 2019

DOI: 10.1021/acs.jced.9b00452
J. Chem. Eng. Data XXXX, XXX, XXX−XXX

Table 1. IUPAC Name, CAS Number, Supplier, Molecular Weight, and Mass Fraction Purity of All Compounds Used

Compound	IUPAC name	CASRN	supplier	molecular weight (g·mol^{-1})	mass fraction purity (wt %)
cholinium hydroxide	2-hydroxyethyl(trimethyl)azanium; hydroxide	123-41-1	Sigma-Aldrich	121.18	46[a]
propanoic acid	propanoic acid	79-09-4	Acros Organics	74.08	99[a]
butanoic acid	butanoic acid	107-92-6	Acros Organics	88.11	99[a]
pentanoic acid	pentanoic acid	109-52-4	Riedel-de Haen	102.13	99[a]
hexanoic acid	hexanoic acid	142-62-1	Sigma-Aldrich	116.16	99.5[a]
heptanoic acid	heptanoic acid	111-14-8	Acros Organics	130.19	99[a]
potassium carbonate	dipotassium;carbonate	584-08-7	Sigma-Aldrich	138.21	>99[a]
[Ch][C_2O_2]	2-hydroxyethyl(trimethyl)azanium; acetate	14586-35-7	Iolitec	163.21	>99[a]
[Ch][C_2CO_2]	2-hydroxy-*N*,*N*,*N*-trimethylethan-1-aminium propionate	n.a.	synthesized in this work	177.24	>97[b]
[Ch][C_3CO_2]	2-hydroxy-*N*,*N*,*N*-trimethylethan-1-aminium butyrate	n.a.	synthesized in this work	191.27	>97[b]
[Ch][C_4CO_2]	2-hydroxy-*N*,*N*,*N*-trimethylethan-1-aminium pentanoate	n.a.	synthesized in this work	205.30	>97[b]
[Ch][C_5CO_2]	2-hydroxy-*N*,*N*,*N*-trimethylethan-1-aminium hexanoate	n.a.	synthesized in this work	219.33	>97[b]
[Ch][C_6CO_2]	2-hydroxy-*N*,*N*,*N*-trimethylethan-1-aminium heptanoate	n.a.	synthesized in this work	233.36	>97[b]
adenine	7*H*-purin-6-amine	73-24-5	Sigma-Aldrich	135.13	99[a]
thymine	5-methyl-1*H*-pyrimidine-2,4-dione	65-71-4	Sigma-Aldrich	126.11	99[a]
cytosine	6-amino-1*H*-pyrimidin-2-one	71-30-7	Sigma-Aldrich	111.10	99[a]
guanine	2-amino-1,7-dihydropurin-6-one	73-40-5	Sigma-Aldrich	151.13	98[a]

[a]Reported by the supplier. [b]Determined by ^{1}H and ^{13}C nuclear magnetic ressonance; n.a., not available.

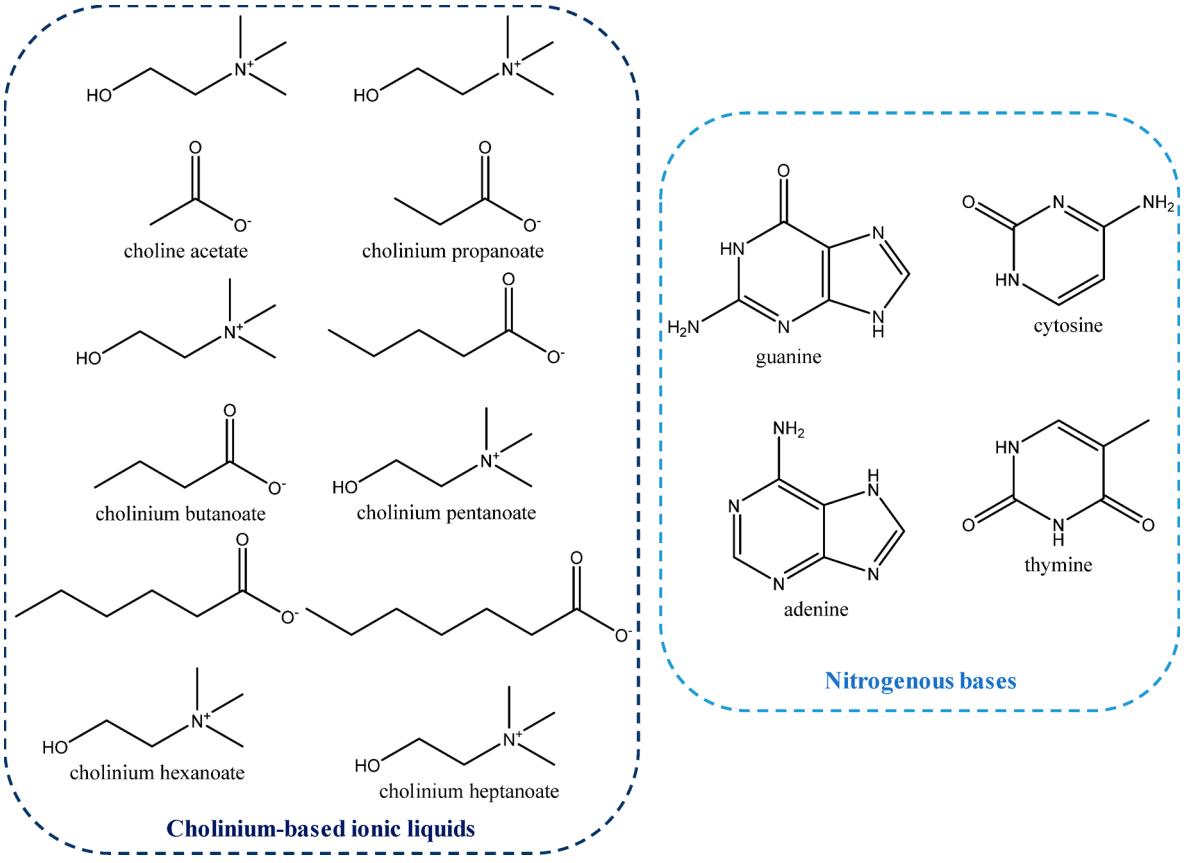

Figure 1. Chemical structures of cholinium-based ILs and nitrogenous bases investigated.

these systems in separation processes, their extraction performance for four nitrogenous bases, namely thymine, adenine, guanine, and cytosine, was then evaluated. These nitrogenous bases are constituents of nucleotides of deoxy-

DOI: 10.1021/acs.jced.9b00452
J. Chem. Eng. Data XXXX, XXX, XXX−XXX

ribonucleic acid (DNA), with their separation being relevant in the biotechnology field.[23,24] However, DNA purification is usually carried out by liquid−liquid extraction involving phenol and chloroform,[25] motivating the development of alternative cost-effective technologies for their purification and for which the data gathered in this work can provide some insights.

EXPERIMENTAL SECTION

Materials. The investigated cholinium-based ILs comprise anions derived from carboxylic acids, namely cholinium acetate ([Ch][C_2O_2]), cholinium propanoate ([Ch][C_2CO_2]), cholinium butanoate ([Ch][C_3CO_2]), cholinium pentanoate ([Ch][C_4CO_2]), cholinium hexanoate ([Ch][C_5CO_2]), and cholinium heptanoate ([Ch][C_6CO_2]). [Ch][C_2O_2] was supplied by Iolitec (>99 wt %). The remaining ILs were synthesized by us following a protocol previously described.[15] The obtained ILs were dried under high vacuum (1 Pa), moderate temperature (313 K), and continuous stirring for at least 72 h. All ILs synthesized showed high purity (>97 wt %), confirmed by ^{1}H and ^{13}C NMR (spectra given in the Supporting Information). The required precursors, namely cholinium hydroxide solution (46 wt %, Sigma-Aldrich), propanoic (99 wt %, Acros Organics), butanoic (99 wt %, Acros Organics), pentanoic (99 wt %, Riedel-de Haen), hexanoic (99.5 wt %, Sigma-Aldrich), and heptanoic acids (99 wt %, Acros Organics), were commercially acquired. The IL-based ABS studied in this work were prepared with potassium carbonate, K_2CO_3 (>99 wt %), purchased from Sigma−Aldrich. For the extraction studies, DNA nitrogenous bases were investigated, namely thymine (99 wt %), adenine (99 wt %), guanine (98 wt %), and cytosine (99 wt %), all acquired from Sigma−Aldrich. The water used was double distilled, passed by a reverse osmosis system and further treated with a Milli-Q plus 185 water purification apparatus. The IUPAC name, CAS number, supplier, molecular weight and mass fraction purity of all compounds used are reported in Table 1. The chemical structures of the investigated ILs and nitrogenous bases are given in Figure 1.

Phase Diagrams and NRTL Modeling. The binodal data were determined through the cloud point titration method at T = (298 ± 1) K and atmospheric pressure. The experimental method used follows the one previously described.[26,27] An aqueous solution of K_2CO_3 at 50 wt % and aqueous solutions of the different ILs at 60 wt % were prepared and used for the determination of the binodal curves. The repetitive dropwise addition of the salt aqueous solution into the aqueous solutions of each IL was carried out until the detection of a cloudy (biphasic) solution, followed by the dropwise addition of ultrapure water until the observation of a limpid solution (monophasic region). All additions were made under continuous stirring. The binodal curves were determined by the weight quantification of all components added ($u(m)$ = 10^{-4} g), in which the weight mass fractions corresponding to the cloud and limpid points were used to describe each binodal curve. The experimental solubility curves were correlated using eq 1:[28]

$$[\mathrm{IL}] = A\,\exp[(B[\mathrm{salt}]^{0.5}) - (C[\mathrm{salt}]^3)] \quad (1)$$

where IL and salt represent the IL and salt weight fraction percentages, respectively, and A, B, and C are constants obtained by regression.

This equation was adopted in this work since it is the most used and requires a lower number of adjustable parameters to correlate the experimental data when compared with other alternatives.[3] Furthermore, this equation allows the direct determination of the tie-lines (TLs) through a mathematical approach (mass balance and lever-arm rule), as proposed by Merchuk et al.[28] Accordingly, ternary mixtures composed of IL + K_2CO_3 + water chosen at the biphasic region were gravimetrically prepared ($u(m)$ = 10^{-4} g) and vigorously agitated. After stirring, the system was allowed to equilibrate for at least 12 h at (298 ± 1) K aiming at the complete separation of the coexisting phases. At this point, both phases were carefully separated and individually weighed. At the conditions used in this work, all systems present the IL-rich phase at the top phase while the salt-rich phase corresponds to the bottom phase.

Each TL was determined through a mathematical approach (mass balance and lever-arm rule), applying a system of six eqs (eqs 2 to 7). Equations 2 and 3 correspond to the description of the binodal curve given by eq 1, yet describing the top and bottom phases, respectively; eqs 4 and 5 correspond to the lever-arm rule; and eqs 6 and 7 correspond to the mass balance of the two ABS phase-forming components, namely the IL and salt. Equations 1 to 5 were previously proposed by Merchuk et al.,[28] whereas eqs 6 and 7 are the salt and IL mass balance added to improve the TL data accuracy. The system of equations used for the TLs determination has four unknown parameters ($[\mathrm{IL}]_T$, $[\mathrm{IL}]_B$, $[\mathrm{salt}]_T$, $[\mathrm{salt}]_B$) and is defined as follows:

$$[\mathrm{IL}]_T = A\,\exp[(B[\mathrm{salt}]_T^{0.5}) - (C[\mathrm{salt}]_T^3)] \quad (2)$$

$$[\mathrm{IL}]_B = A\,\exp[(B[\mathrm{salt}]_B^{0.5}) - (C[\mathrm{salt}]_B^3)] \quad (3)$$

$$[\mathrm{salt}]_T = \frac{[\mathrm{IL}]_M}{\alpha} - \frac{1-\alpha}{\alpha}[\mathrm{IL}]_B \quad (4)$$

$$[\mathrm{salt}]_B = \frac{[\mathrm{salt}]_M}{\alpha} - \frac{1-\alpha}{\alpha}\cdot[\mathrm{salt}]_B \quad (5)$$

$$m_M^{\mathrm{IL}} = m_T[\mathrm{IL}]_T + m_B[\mathrm{IL}]_B \quad (6)$$

$$m_M^{\mathrm{salt}} = m_T\cdot[\mathrm{salt}]_T + m_B\cdot[\mathrm{salt}]_B \quad (7)$$

where m is the mass of component i (IL or salt) and the subscripts M, T, and B designate, respectively, the initial mixture, the top and bottom phases. The value α is the ratio between the mass of the top phase and the total mass of the mixture experimentally determined. Finally, the tie-line length (TLL) was determined through the application of the following equation:

$$\mathrm{TLL} = \sqrt{([\mathrm{salt}]_T - [\mathrm{salt}]_B)^2 + ([\mathrm{IL}]_T - [\mathrm{IL}]_B)^2} \quad (8)$$

To ascertain the reliability of the TLs determined by the application of eqs 1 to 7 and to address the possibility of ion exchange in the investigated systems, the IL cation ($[\mathrm{Ch}]^+$) and anion ($[\mathrm{C}_n\mathrm{CO}_2]^-$) in the IL-(top)-rich phase were quantified by ^{1}H NMR (Bruker AMX 300), operating at 300 MHz, by integrating the peak area of the analyte with that of a reference. Benzene was used as an external standard, the solution of which was gravimetrically prepared in a DMSO sealed capillary, and further validated against several standards. The ^{1}H NMR peak corresponding to the hydrogens of the three methyl groups of the cholinium was used to quantify the

DOI: 10.1021/acs.jced.9b00452
J. Chem. Eng. Data XXXX, XXX, XXX−XXX

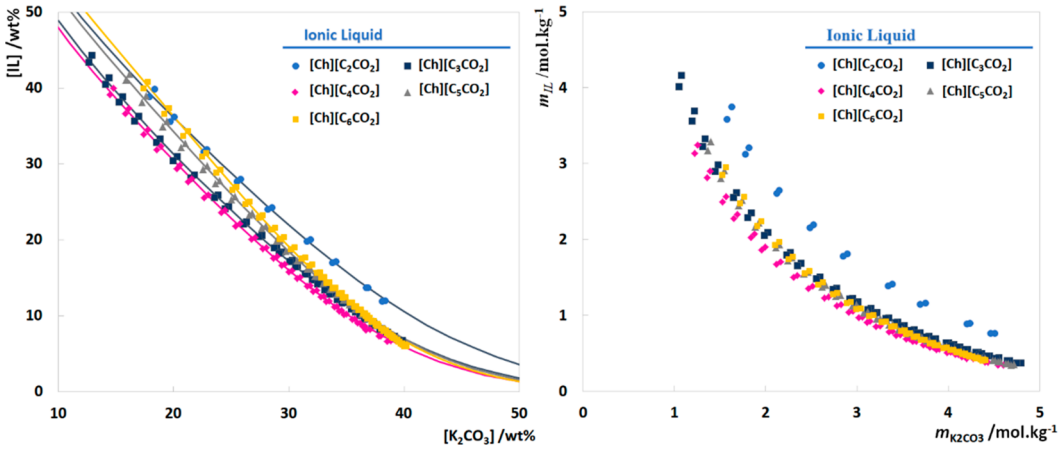

Figure 2. Orthogonal phase diagram representation for the ABS formed by IL + K_2CO_3 + water at (298 ± 1) K and atmospheric pressure. The solid lines represent the fitting by eq 1.

IL cation while the hydrogens from the last carbon of the alkyl chain of the anion were used to quantify the IL anion (cf. NMR spectra given in the Supporting Information). Two mixture compositions of each ABS comprising $[Ch][C_2CO_2]$, $[Ch][C_3CO_2]$, or $[Ch][C_4CO_2]$, corresponding to the same mixture compositions used and where eqs 1 to 7 were applied, were prepared and the IL cation and anion quantified at the IL-rich phase. These three ILs were selected since the ABS formed by $[Ch][C_2CO_2]$ + K_2CO_3 + water has the smallest biphasic region whereas $[Ch][C_4CO_2]$ + K_2CO_3 + water has the largest biphasic region, with the binodal curve of the system comprising $[Ch][C_3CO_2]$ falling between.

The liquid−liquid equilibrium data experimentally determined was modeled using the local composition activity model nonrandom two-liquid (NRTL).[29] The NRTL model is known to be robust and flexible enough for modeling both ternary LLE data and binary subsystems using a common parameter set—the binary interaction parameters τ_{ij}. Several works have shown the adequacy of using the NRTL model to describe organic−IL binary mixtures, as well as salt−IL or polymer−salt ABS.[30−36] However, determining these parameters set by fitting the model to ternary experimental TLs may lead to poor descriptions of the binary subsystems. To the best of our knowledge no binary interaction parameters exist for the studied binary subsystems.

Aiming at minimizing the loss of the model parameters physical meaning, NRTL parameters were optimized by the simultaneous regression of the following equations to all the experimental data available (five ternary systems and three tie-lines per system) using the objective function OF:

$$x_i^{\mathrm{T}}\gamma_i^{\mathrm{T}} = x_i^{\mathrm{B}}\gamma_i^{\mathrm{B}} \tag{9}$$

$$\ln(\gamma_i) = \frac{\sum_j \tau_{ji}G_{ji}x_j}{\sum_k G_{ki}x_k} + \sum_j \left[\frac{x_i G_{ij}}{\sum_k G_{kj}x_k}\left(\tau_{ij} - \frac{\sum_m \tau_{mj}G_{mj}x_m}{\sum_k G_{kj}x_k}\right)\right] \tag{10}$$

$$G_{ij} = \exp(-\alpha_{ij}\tau_{ij}) \tag{11}$$

$$\mathrm{OF} = \sum_p \sum_n \sum_k (x_{p,n,k}^{\mathrm{exp}} - x_{p,n,k}^{\mathrm{calc}})^2 \tag{12}$$

where τ_{ij} are the $i-j$ interactions parameters, α_{ij} is related to the nonrandomness of the mixture, and the common value of 0.3 was taken as default for all systems.

The estimation of the critical point of the studied systems was determined using the following equation,[37]

$$[\mathrm{IL}] = D + E[K_2CO_3] \tag{13}$$

were D and E are the fitting parameters.

Extraction of Nitrogenous Bases. From the phase diagrams determined in this work, ternary mixture compositions which lead to the formation of two-phase systems were chosen to carry out the extraction of nitrogenous bases. To avoid discrepancies that may result from differences in composition between the two phases, all extraction studies were performed at a similar TLL (ca. 56 ± 2). Aqueous solutions of thymine, adenine, and cytosine were prepared at a concentration of 0.80 mg·mL^{-1} and added according to the water content in each ABS, resulting in a concentration ranging between 0.34 and 0.38 mg·mL^{-1} in the overall system. For the guanine extraction, and due to its low water-solubility, 1 mg of the nitrogenous base was added directly to each ABS, resulting in a concentration around 0.5 mg·mL^{-1} in the overall system. Each mixture was vigorously stirred, centrifuged for 30 min at (298 ± 1) K to reach the nitrogenous bases equilibrium and partition between the coexisting phases. After, a careful separation of the phases was performed, and each nitrogenous base in each phase was quantified by UV-spectroscopy, using a BioTeck Synergy HT microplate reader at a wavelength of 260 nm, using calibration curves previously established. At least three independent ABS were prepared, and three samples of each phase were quantified. Control or "blank" solutions at the same mixture point used for the extraction studies (with no nitrogenous bases added) were used in all systems.

The percentage extraction efficiencies of each ABS to each nitrogenous base, EE%, are defined as the percentage ratio between the amount of each nitrogenous base in the IL-rich aqueous phase and that in the total mixture, according to eq 14:

$$\mathrm{EE_{NB}}\% = \frac{w_{\mathrm{NB}}^{\mathrm{IL}}}{w_{\mathrm{NB}}^{\mathrm{IL}} + w_{\mathrm{NB}}^{\mathrm{salt}}}100 \tag{14}$$

DOI: 10.1021/acs.jced.9b00452
J. Chem. Eng. Data XXXX, XXX, XXX−XXX

where w_{NB}^{IL} and w_{NB}^{salt} are the total weight of each nitrogen base (NB) in the IL-rich and in the salt-rich aqueous phases, respectively.

The pH of each ABS phase was measured at (298 ± 1) K using a Mettler Toledo S47 Seven MultiTM dual meter pH instrument.

RESULTS

Phase Diagrams and NRTL Modeling. Novel ternary phase diagrams for five ILs ([Ch][C_2CO_2], [Ch][C_3CO_2], [Ch][C_4CO_2], [Ch][C_5CO_2], and [Ch][C_6CO_2]) + K_2CO_3 + water were determined at (298 ± 1) K and atmospheric pressure. Although [Ch][C_2O_2] was also tested, this IL does not form ABS with K_2CO_3 due to its higher hydrophilicity, thus requiring stronger salting-out species to induce phase separation. The experimental weight fraction data of each phase diagram are reported in the Supporting Information, whereas the respective phase diagrams are displayed in Figure 2. The phase diagrams are represented in an orthogonal representation in which the water content corresponds to the difference needed to reach 100 wt %. The fitting of the experimental data by eq 1 is also shown in Figure 2. The regression parameters were estimated by the least-squares regression method, and their values and corresponding standard deviations (σ) are provided in Table 2. The solubility curves are presented in both weight fraction and molality units. The latter representation is used to better understand the impact of each IL on the phase diagram behavior, avoiding differences that would result from different molecular weights, and particularly relevant regarding the effect of the ILs self-aggregation when dealing with ILs with longer alkyl side chains at the anion.

Table 2. Adjusted Parameters and Respective Standard Deviations (σ) Obtained by Fitting of the Experimental Data by eq 1

IL	$A \pm \sigma$	$B \pm \sigma$	10^5 ($C \pm \sigma$)
[Ch][C_2CO_2]	(106.6 ± 8.7) × 10^{-6}	−0.225 ± 0.004	1.49 ± 0.09
[Ch][C_3CO_2]	105.5 ± 7.6	−0.237 ± 0.019	1.91 ± 0.11
[Ch][C_4CO_2]	102.0 ± 10.3	−0.232 ± 0.026	2.17 ± 0.14
[Ch][C_5CO_2]	(101.9 ± 4.8) × 10^{-6}	−0.205 ± 0.002	2.19 ± 0.04
[Ch][C_6CO_2]	(100.0 ± 6.4) × 10^{-6}	−0.184 ± 0.002	2.41 ± 0.04

Phase diagrams shown in Figure 2 with a larger area above the solubility curve display higher ability to form two phases, that is, required lower amounts of salt or IL to create two-phase systems. Accordingly, the ability of cholinium-ILs to form ABS at (298 ± 1) K at 2.0 mol·kg^{-1} follows the rank: [Ch][C_4CO_2] > [Ch][C_3CO_2] ≈ [Ch][C_5CO_2] ≈ [Ch][C_6CO_2] > [Ch][C_2CO_2]. Although this order shows that the capability to form ABS (or of the IL to be salted-out) increases with the increase of the alkyl chain length of the IL anion, this is only observed up to cholinium pentanoate; for higher anion alkyl chain lengths the self-aggregation of the ILs occurs, decreasing their ability to create ABS.[38,39] This trend in ABS formation is in agreement with what has been recently observed for cholinium-based ILs + K_2HPO_4 ABS and seems to be independent of the salt used.[40] Moreover, the same trend was previously reported for the IL cation effect in ABS formation.[41]

Three mixture compositions at the biphasic region of each ABS were prepared, and eqs 1 to 7 were applied to determine the respective TLs, along with their respective length (TLLs), which are reported in Table 3. The critical points determined for the studied systems are reported in Figure 3. The IL cation and anion in the IL-rich phase of different TLs were quantified by ^{1}H NMR to address the reliability of applying eqs 1 to 7 since ion exchange may occur. The results obtained are given in the Supporting Information. Although two salts are used in the investigated ABS, the results obtained demonstrate that the IL cation and anion at the IL-rich phase exist in a ratio of 1:1, proving that ion exchange in these systems does not exist or, if it exists, it is of low significance and below the detection limit of the analytical technique. These results confirm the reliability of the TLs given in Table 3.

Even though there are several ions in solution, ion exchange between the salt and IL ions in the ABS investigated appear to be not relevant since the different ions will have a low probability to create different ion pairs (the salt used is composed of high-charge density ions, whereas the IL is constituted by low-charge density ions). Previous works addressed this possibility.[42,43] It should be however remarked that ion exchange is more significant when dealing with ILs mixtures.[44]

The NRTL activity coefficient model was applied to the TL data aiming at proposing binary interaction parameters capable of describing the systems under study. The determination of the binary interaction parameters by fitting the model only to ternary experimental LLE data may lead to poor descriptions of the binary subsystems. Aiming at minimizing the loss of the model parameters physical meaning, the NRTL parameters were optimized by simultaneously regressing all the experimental data (five ternary systems and three tie-lines per system) using the objective function given by eq 12. To the best of our knowledge no binary interaction parameters exist for the studied binary subsystems using the NRTL activity coefficient model. As depicted in Figure 3, the set of optimized binary interaction parameters allows an excellent description of the experimental data with a %AAD (average absolute deviation) of 5.57 × 10^{-4}, calculated as

$$\%AAD = \sum_{i}^{N} \left| \frac{w\%_{exp} - w\%_{calc}}{w\%_{exp}} \right| 100/N$$

The IL-rich phase nonideality is governed by the IL and water interactions while at the salt-rich phase the nonideality of the ABS is governed by the water and salt interactions—as demonstrated by the activity coefficients given in the Supporting Information and the binary interaction parameters depicted in Figure 3. The nonideality observed is a clear indication that upon mixing of the three components the interactions that the salt establishes with water compete with those present in the IL + water binary system, promoting liquid−liquid equilibrium.

Extraction of Nitrogenous Bases. The preferential migration of biomolecules in ABS may be dependent on specific interactions or on their affinity for a given phase according to the coexisting phases polarities, which can be achieved by changing the IL used in the ABS. The effect of the cholinium-based IL ([Ch][C_2CO_2], [Ch][C_3CO_2], [Ch][C_4CO_2], [Ch][C_5CO_2], and [Ch][C_6CO_2]) in the partition-

DOI: 10.1021/acs.jced.9b00452
J. Chem. Eng. Data XXXX, XXX, XXX−XXX

Table 3. Weight Fraction Compositions (wt%) of the Initial Mixture (*M*), TL Data Given by the Compositions of the Top (*T*, IL-Rich) and Bottom (*B*, Salt-Rich) Phases, and TLLs of the ABS Composed of Water + Cholinium-Based ILs + K_2CO_3 at (298 ± 1) K and Atmospheric Pressure (0.1 MPa).[a]

	weight fraction composition/wt %						
IL	$[IL]_T$	$[salt]_T$	$[IL]_M$	$[salt]_M$	$[IL]_B$	$[salt]_B$	TLL
$[Ch][C_2CO_2]$	41.71	16.44	26.01	29.73	4.79	47.67	48.36
	46.44	13.61	26.10	31.06	3.35	50.56	56.76
	48.75	12.31	26.23	31.93	2.57	52.54	61.24
$[Ch][C_3CO_2]$	41.50	13.84	26.12	26.07	4.92	42.90	46.72
	43.01	13.01	25.77	27.22	3.46	45.61	51.25
	45.80	11.53	26.27	28.06	2.34	48.31	56.93
$[Ch][C_4CO_2]$	39.70	14.39	25.61	26.04	3.19	44.57	47.38
	44.28	11.86	25.83	27.21	2.26	46.84	54.67
	48.78	9.61	26.51	27.86	1.84	48.08	60.69
$[Ch][C_5CO_2]$	43.50	14.64	26.36	27.85	3.15	45.76	50.96
	46.85	12.78	25.99	28.87	2.64	46.88	55.82
	51.06	10.57	26.00	30.29	1.75	49.37	62.75
$[Ch][C_6CO_2]$	37.02	19.39	29.88	25.14	1.94	47.49	44.96
	43.59	15.08	30.09	26.19	1.18	50.00	54.94
	46.21	13.22	29.80	27.34	0.70	52.37	60.03

[a]The combined standard uncertainty for the weight fraction $u_r(w)$ is 0.01, the standard uncertainty for the temperature $u(T)$ is 1 K, and the standard uncertainty for pressure $u(p)$ is 10 kPa.

ing of DNA nitrogenous bases, namely thymine, adenine, guanine, and cytosine, in ABS formed by water + IL + K_2CO_3 was evaluated at (298 ± 1) K at a common TLL (ca. 56 ± 2). The mixture compositions, respective phases' compositions, and TLLs are presented in Table 3. The extraction efficiencies (EE_{NB}%) of nitrogenous bases with different ABS are shown in Figure 4, the detailed results of which are given in the Supporting Information.

In all systems, DNA nitrogenous bases preferentially migrate to the most hydrophobic phase, that is, the IL-rich phase, with extraction efficiencies ranging between 81% and 97% achieved in a single-step. These values support the salting-out effect exerted by K_2CO_3 and/or the preferential affinity of the studied DNA nitrogenous bases to the IL-rich phase (low water content; cf. Table 3). When the respective standard deviations are taken into account, there are no significant differences on the extraction efficiencies by each IL-based ABS to the same nitrogenous base. Since all extraction experiments were carried out at a similar TLL, where the differences between the coexisting phase's compositions are kept equal, this trend reflects the absence of specific interactions arising from the IL alkyl side chain length increase and the studied nitrogenous bases.

The extraction efficiencies of most studied ABS to each DNA nitrogenous base, as displayed in Figure 4 and taking into account the associated standard deviations, decrease in the following order: adenine > thymine > cytosine > guanine. This ranking correlates with the logarithm of the octanol−water partition coefficients ($\log(K_{ow})$) of the investigated nitrogenous bases (adenine, −0.05; thymine, −0.62; cytosine, −1.48; and guanine, −1.77),[45] where the most hydrophobic bases partition in a more extensive way to the IL-rich phase. These results are in agreement with the discussion provided above—the studied bases preferentially partition to the most hydrophobic (IL-rich) phase.

The studied nitrogen bases suffer speciation according to the ABS pH values. The pH values of both top and bottom phases are given in the Supporting Information, and range between 11.8 and 12.4. The dissociation curves of thymine, adenine, guanine, and cytosine as a function of pH[46] are provided in the Supporting Information. According to the pH values of the IL- and K_2CO_3-rich phases, the nitrogenous bases thymine, adenine, and cytosine have a charge of −1, while guanine has a charge of −2, and thus could interact with the IL cholinium cation. However, since significant differences in the extraction efficiencies occur between nitrogenous bases with the same charge and no significant changes are observed with different ILs, which will have an impact through different cation−anion interaction strengths, it seems that electrostatic interactions between the IL cation and each base do not play a relevant role.

To the best of our knowledge, no studies on the use of IL-based ABS to extract nitrogenous bases of nucleotides from DNA have been reported in the literature; however, some works reporting on the use of ABS for the extraction of DNA can be found in the literature.[47−49] Huang and Huang[49] used ABS composed of the 1-butyl-3-methylimidazolium tetrafluoroborate and KH_2PO_4 for extracting yeast DNA. Moreover, Xu et al.[48] applied ABS formed by ILs or deep eutectic solvents to extract DNA, with a maximum extraction efficiency of 99.6%. In this work, similar extraction efficiencies were attained for nitrogenous bases from DNA while using cholinium-based ILs, reinforcing the need of studying additional ABS composed of more biocompatible and low cost ILs as alternative separation platforms.

Aiming at developing sustainable separation processes, the recovery of the studied nitrogenous bases from the IL-rich is mandatory and can be carried out using different strategies. Because of the low water solubility of nitrogenous bases in water and taking into account the hydrotropic phenomenon afforded by ILs, the addition of water may lead to the nitrogenous bases precipitation, as proposed by Ferreira et al.[50] and Cláudio et al.[51] The back-extraction of the nitrogenous bases from the IL-rich phase using organic solvents where nitrogenous bases are more soluble is also a possible strategy, as carried out by Cláudio et al.[52] Finally, the recovery of the nitrogenous bases by solid-phase extraction using effective

DOI: 10.1021/acs.jced.9b00452
J. Chem. Eng. Data XXXX, XXX, XXX−XXX

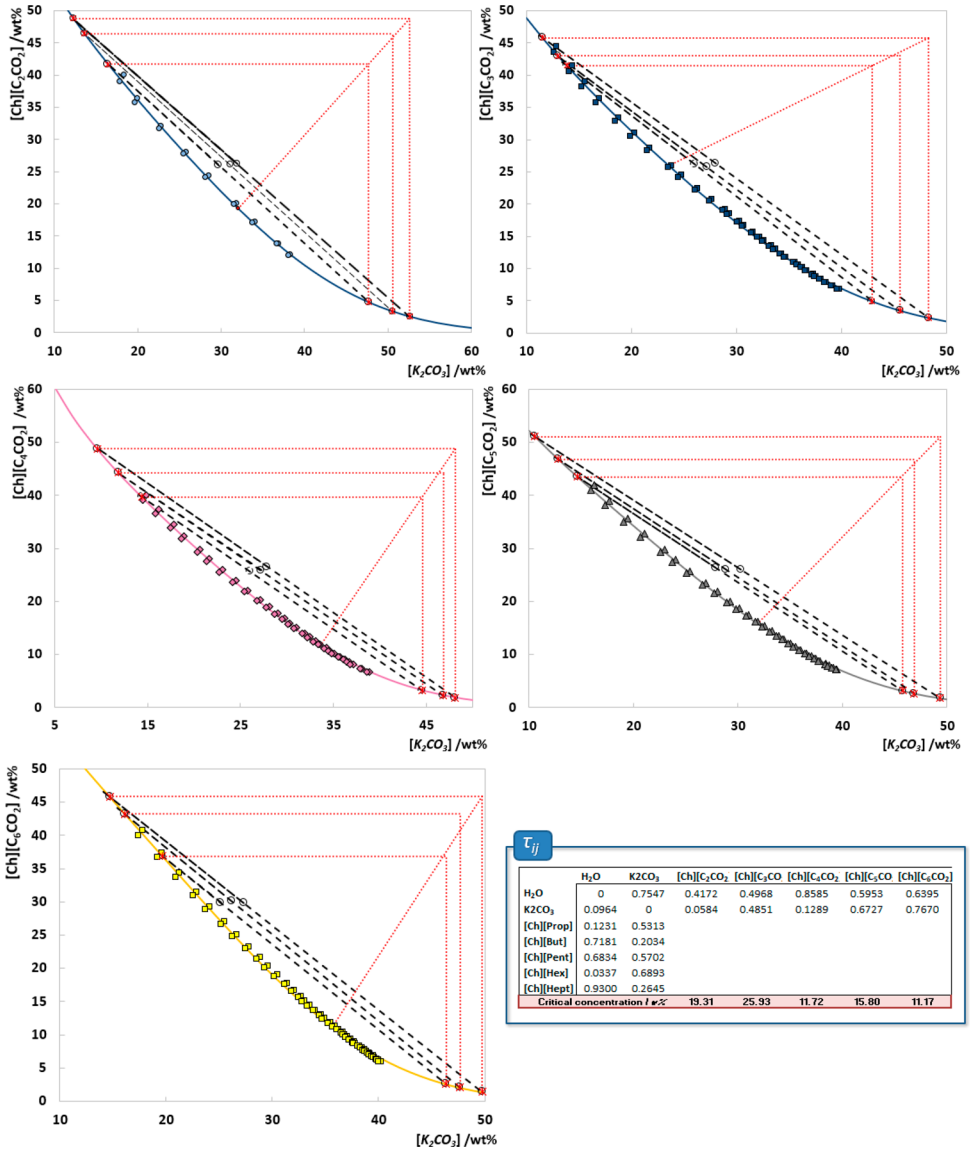

Figure 3. Phase diagrams for the studied ternary systems, optimized NRTL binary interaction parameters, and IL critical concentration: (Solid lines) fitting by eq 1; (red dotted lines) critical point estimation determined by eq 13; (black empty circles) experimental TLs; (red stars) TLs obtained from the NRTL fitting.

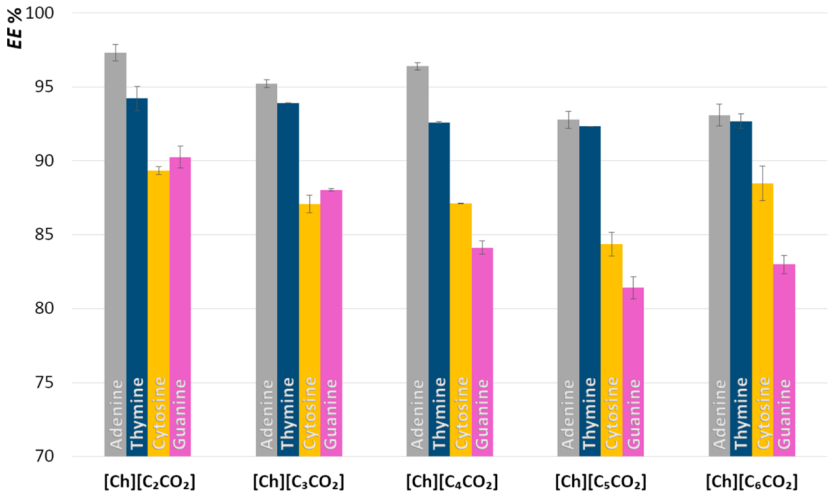

Figure 4. Extraction efficiencies of each ABS to nitrogenous bases (EE_{NB}%) at (298 ± 1) K.

DOI: 10.1021/acs.jced.9b00452
J. Chem. Eng. Data XXXX, XXX, XXX−XXX

cartridges, as those identified by Czarnecka et al.,[53] may be used as an effective recovery approach.

CONCLUSIONS

In this work, novel ternary phase diagrams for ABS composed of water, cholinium-based ILs, and K_2CO_3 at (298 ± 1) K and atmospheric pressure were determined. In addition to each binodal curve, TLs and critical points have been determined, and the NRTL model was applied. The capability to form ABS (or of the IL to be salted-out) increases with the increase of the alkyl chain length of the IL anion up to cholinium pentanoate; nevertheless, for longer anion alkyl chain lengths, the self-aggregation of the ILs leads to a decrease of their ability to form ABS. The set of optimized binary interaction parameters allowed an excellent description of the experimental data by the NRTL model, with a %AAD of 5.57 × 10^{-4}. Furthermore, it is shown that the IL-rich phase nonideality is governed by the IL and water interactions, while at the salt-rich phase the nonideality is governed by the water and salt interactions.

After the characterization of the studied ABS they were finally evaluated, at a fixed TLL (56 ± 2), for the extraction of nitrogenous bases. The systems investigated allow extraction efficiencies ranging from 81% to 97% to the IL-rich phase in a single-step. Taking into account the respective standard deviations, no significant differences on the extraction efficiencies by each IL-based ABS to the same nitrogenous base were found, reinforcing the absence of specific interactions arising from the IL alkyl side chain length increase and the studied nitrogenous bases since all experiments were carried out at a similar TLL. On the other hand, more significant differences are seen when addressing the same IL-based ABS to extract different bases. In general, it was found that the most hydrophobic bases partition in a more extensive way to the IL-rich phase, following the respective octanol–water partition coefficients.

The novel set of results here presented contribute to a better characterization of IL-based ABS composed of cholinium carboxylate ILs and salts, while foreseeing their application in the separation of value-added compounds.

ASSOCIATED CONTENT

Supporting Information

The Supporting Information is available free of charge on the ACS Publications website at DOI: 10.1021/acs.jced.9b00452.

IL NMR data, experimental weight fraction data, IL cation and anion content in the IL-rich phase determined by NMR, NRTL activity coefficients, dissociation curves of nitrogenous bases, extraction efficiencies (PDF)

AUTHOR INFORMATION

Corresponding Author

*Tel.: +351-234-370200. Fax: +351-234-370084. E-mail: maragfreire@ua.pt.

ORCID

Pedro J. Carvalho: 0000-0002-1943-0006

Mara G. Freire: 0000-0001-8895-0614

Notes

The authors declare no competing financial interest.

ACKNOWLEDGMENTS

This work was developed within the scope of the project CICECO-Aveiro Institute of Materials, FCT ref. UID/CTM/50011/2019, financed by national funds through the FCT/MCTES. D.C.V.B. acknowledges the financial support from Conselho Nacional de Desenvolvimento Científico e Tecnológico CNPq for the Ph.D. grant (202337/2015-4). P.J.C. acknowledges the FCT/MCTES for a research contract (IF/00758/2015) under the Program "Investigador FCT".

REFERENCES

(1) Gutowski, K. E.; Broker, G. A.; Willauer, H. D.; Huddleston, J. G.; Swatloski, R. P.; Holbrey, J. D.; Rogers, R. D. Controlling the aqueous miscibility of ionic liquids: aqueous biphasic systems of water-miscible ionic liquids and water-structuring salts for recycle, metathesis, and separations. *J. Am. Chem. Soc.* **2003**, *125*, 6632–3.

(2) Quental, M. V.; Passos, H.; Kurnia, K. A.; Coutinho, J. A. P.; Freire, M. G. Aqueous Biphasic Systems Composed of Ionic Liquids and Acetate-Based Salts: Phase Diagrams, Densities, and Viscosities. *J. Chem. Eng. Data* **2015**, *60*, 1674–1682.

(3) Freire, M. G.; Claudio, A. F.; Araujo, J. M.; Coutinho, J. A. P.; Marrucho, I. M.; Canongia Lopes, J. N.; Rebelo, L. P. Aqueous biphasic systems: a boost brought about by using ionic liquids. *Chem. Soc. Rev.* **2012**, *41*, 4966–95.

(4) Ventura, S. P. M.; Sousa, S. G.; Freire, M. G.; Serafim, L. S.; Lima, Á. S.; Coutinho, J. A. P. Design of ionic liquids for lipase purification. *J. Chromatogr. B: Anal. Technol. Biomed. Life Sci.* **2011**, *879*, 2679–2687.

(5) Pei, Y.; Wang, J.; Liu, L.; Wu, K.; Zhao, Y. Liquid–Liquid Equilibria of Aqueous Biphasic Systems Containing Selected Imidazolium Ionic Liquids and Salts. *J. Chem. Eng. Data* **2007**, *52*, 2026–2031.

(6) Gómez, E.; Domínguez, I.; Domínguez, Á.; Macedo, E. A. Ionic Liquids-Based Aqueous Biphasic Systems with Citrate Biodegradable Salts. *J. Chem. Eng. Data* **2018**, *63*, 1103–1108.

(7) Pereira, J. F.; Lima, Á. S.; Freire, M. G.; Coutinho, J. A. P. Ionic liquids as adjuvants for the tailored extraction of biomolecules in aqueous biphasic systems. *Green Chem.* **2010**, *12*, 1661–1669.

(8) João, K. G.; Tomé, L. C.; Gouveia, A. S. L.; Marrucho, I. M. Aqueous Biphasic Systems of Pyrrolidinium Ionic Liquids with Organic Acid-Derived Anions and K3PO4. *J. Chem. Eng. Data* **2017**, *62*, 1182–1188.

(9) Gao, J.; Chen, L.; Yan, Z. Phase Behavior of Aqueous Biphasic Systems Composed of Ionic Liquids and Organic Salts. *J. Chem. Eng. Data* **2015**, *60*, 464–470.

(10) Chen, Y.; Meng, Y.; Yang, J.; Li, H.; Liu, X. Phenol Distribution Behavior in Aqueous Biphasic Systems Composed of Ionic Liquids–Carbohydrate–Water. *J. Chem. Eng. Data* **2012**, *57*, 1910–1914.

(11) Wang, R.; Chang, Y.; Tan, Z.; Li, F. Phase behavior of aqueous biphasic systems composed of novel choline amino acid ionic liquids and salts. *J. Mol. Liq.* **2016**, *222*, 836–844.

(12) Liu, X.; Yang, Q.; Bao, Z.; Su, B.; Zhang, Z.; Ren, Q.; Yang, Y.; Xing, H. Nonaqueous Lyotropic Ionic Liquid Crystals: Preparation, Characterization, and Application in Extraction. *Chem. - Eur. J.* **2015**, *21*, 9150–9156.

(13) Shahriari, S.; Tomé, L. C.; Araújo, J. M.; Rebelo, L. P. N.; Coutinho, J. A. P.; Marrucho, I. M.; Freire, M. G. Aqueous biphasic systems: a benign route using cholinium-based ionic liquids. *RSC Adv.* **2013**, *3*, 1835–1843.

(14) Santos, J.; Goncalves, A.; Pereira, J.; Figueiredo, B.; e Silva, F.; Coutinho, J. A. P.; Ventura, S. P. M.; Goncalves, F. Environmental safety of cholinium-based ionic liquids: assessing structure–ecotoxicity relationships. *Green Chem.* **2015**, *17*, 4657–4668.

(15) Quental, M. V.; Caban, M.; Pereira, M. M.; Stepnowski, P.; Coutinho, J. A. P.; Freire, M. G. Enhanced extraction of proteins using cholinium-based ionic liquids as phase-forming components of aqueous biphasic systems. *Biotechnol. J.* **2015**, *10*, 1457–1466.

DOI: 10.1021/acs.jced.9b00452
J. Chem. Eng. Data XXXX, XXX, XXX–XXX

(16) Song, C. P.; Ramanan, R. N.; Vijayaraghavan, R.; MacFarlane, D. R.; Chan, E.-S.; Ooi, C.-W. Green, aqueous two-phase systems based on cholinium aminoate ionic liquids with tunable hydrophobicity and charge density. *ACS Sustainable Chem. Eng.* **2015**, *3*, 3291−3298.
(17) Taha, M.; Quental, M. V.; Correia, I.; Freire, M. G.; Coutinho, J. A. P. Extraction and stability of bovine serum albumin (BSA) using cholinium-based Good's buffers ionic liquids. *Process Biochem.* **2015**, *50*, 1158−1166.
(18) Taha, M.; Almeida, M. R.; Silva, F. A. e.; Domingues, P.; Ventura, S. P. M.; Coutinho, J. A. P.; Freire, M. G. Novel biocompatible and self-buffering ionic liquids for biopharmaceutical applications. *Chem. - Eur. J.* **2015**, *21*, 4781−4788.
(19) Requejo, P. F.; Gómez, E.; Macedo, E. A. Partitioning of DNP-Amino Acids in New Biodegradable Choline Amino Acid/Ionic Liquid-Based Aqueous Two-Phase Systems. *J. Chem. Eng. Data* **2019**, DOI: 10.1021/acs.jced.9b00052.
(20) Li, Z.; Liu, X.; Pei, Y.; Wang, J.; He, M. Design of environmentally friendly ionic liquid aqueous two-phase systems for the efficient and high activity extraction of proteins. *Green Chem.* **2012**, *14*, 2941−2950.
(21) Liu, X.; Li, Z.; Pei, Y.; Wang, H.; Wang, J. Liquid+liquid) equilibria for (cholinium-based ionic liquids+polymers) aqueous two-phase systems. *J. Chem. Thermodyn.* **2013**, *60*, 1−8.
(22) Pereira, J. F.; Kurnia, K. A.; Cojocaru, O. A.; Gurau, G.; Rebelo, L. P. N.; Rogers, R. D.; Freire, M. G.; Coutinho, J. A. P. Molecular interactions in aqueous biphasic systems composed of polyethylene glycol and crystalline vs. liquid cholinium-based salts. *Phys. Chem. Chem. Phys.* **2014**, *16*, 5723−5731.
(23) Ferraro, B.; Morrow, M. P.; Hutnick, N. A.; Shin, T. H.; Lucke, C. E.; Weiner, D. B. Clinical applications of DNA vaccines: current progress. *Clin. Infect. Dis.* **2011**, *53*, 296−302.
(24) Fang, J.; Zhu, X.; Wang, C.; Shangguan, L. Applications of DNA Technologies in Agriculture. *Curr. Genomics* **2016**, *17*, 379−386.
(25) Liu, D. *Handbook of nucleic acid purification*; CRC Press, 2009.
(26) Ventura, S. P. M.; Sousa, S. G.; Serafim, L. S.; Lima, Á. S.; Freire, M. G.; Coutinho, J. A. P. Ionic liquid based aqueous biphasic systems with controlled pH: the ionic liquid cation effect. *J. Chem. Eng. Data* **2011**, *56*, 4253−4260.
(27) Neves, C. M.; Ventura, S. P. M.; Freire, M. G.; Marrucho, I. M.; Coutinho, J. A. P. Evaluation of cation influence on the formation and extraction capability of ionic-liquid-based aqueous biphasic systems. *J. Phys. Chem. B* **2009**, *113*, 5194−5199.
(28) Merchuk, J. C.; Andrews, B. A.; Asenjo, J. A. Aqueous two-phase systems for protein separation: studies on phase inversion. *J. Chromatogr., Biomed. Appl.* **1998**, *711*, 285−293.
(29) Renon, H.; Prausnitz, J. M. Estimation of Parameters for the NRTL Equation for Excess Gibbs Energies of Strongly Nonideal Liquid Mixtures. *Ind. Eng. Chem. Process Des. Dev.* **1969**, *8*, 413−419.
(30) Haghtalab, A.; Paraj, A. Computation of liquid−liquid equilibrium of organic-ionic liquid systems using NRTL, UNIQUAC and NRTL-NRF models. *J. Mol. Liq.* **2012**, *171*, 43−49.
(31) Simoni, L. D.; Lin, Y.; Brennecke, J. F.; Stadtherr, M. A. Modeling Liquid−Liquid Equilibrium of Ionic Liquid Systems with NRTL, Electrolyte-NRTL, and UNIQUAC. *Ind. Eng. Chem. Res.* **2008**, *47*, 256−272.
(32) Zafarani-Moattar, M. T.; Sadeghi, R. Measurement and correlation of liquid−liquid equilibria of the aqueous two-phase system polyvinylpyrrolidone−sodium dihydrogen phosphate. *Fluid Phase Equilib.* **2002**, *203*, 177−191.
(33) Zafarani-Moattar, M. T.; Hamzehzadeh, S. Liquid−liquid equilibria of aqueous two-phase systems containing polyethylene glycol and sodium succinate or sodium formate. *CALPHAD: Comput. Coupling Phase Diagrams Thermochem.* **2005**, *29*, 1−6.
(34) Sadeghi, R. Measurement and correlation of phase equilibria for several PVP+ salt aqueous two-phase systems at 303.15 K. *Fluid Phase Equilib.* **2005**, *237*, 40−47.
(35) Zafarani-Moattar, M. T.; Hamzehzadeh, S. Liquid−Liquid Equilibria of Aqueous Two-Phase Systems Containing 1-Butyl-3-methylimidazolium Bromide and Potassium Phosphate or Dipotassium Hydrogen Phosphate at 298.15 K. *J. Chem. Eng. Data* **2007**, *52*, 1686−1692.
(36) Zafarani-Moattar, M. T.; Shekaari, H.; Jafari, P. Liquid-liquid equilibria of choline chloride + 1-propanol or 2-propanol + water ternary systems at different temperatures: Study of choline chloride ability for recovering of these alcohols from water mixtures. *J. Mol. Liq.* **2019**, *273*, 463−475.
(37) Lee, B. H.; Qin, Y.; Prausnitz, J. M. Thermodynamic representation of ternary liquid−liquid equilibria near-to and far-from the plait point. *Fluid Phase Equilib.* **2006**, *240*, 67−72.
(38) Xie, Y.; Xing, H.; Yang, Q.; Bao, Z.; Su, B.; Ren, Q. Aqueous biphasic system containing long chain anion-functionalized ionic liquids for high-performance extraction. *ACS Sustainable Chem. Eng.* **2015**, *3*, 3365−3372.
(39) Patidar, P.; Bahadur, A.; Prasad, K.; Tiwari, S.; Aswal, V. K.; Bahadur, P. Synthesis, self-assembly and micellization characteristics of choline alkanoate ionic liquids in association with a star block copolymer. *Colloids Surf., A* **2018**, *555*, 691−698.
(40) Belchior, D. C.; Almeida, M. R.; Sintra, T. E.; Ventura, S. P. M.; Duarte, I. F.; Freire, M. G. Odd-even effect in the formation and extraction performance of ionic-liquid-based aqueous biphasic systems. *Ind. Eng. Chem. Res.* **2019**, *58*, 8323.
(41) Belchior, D. C.; Sintra, T. E.; Carvalho, P. J.; Soromenho, M. R.; Esperança, J. M.; Ventura, S. P. M.; Rogers, R. D.; Coutinho, J. A. P.; Freire, M. G. Odd-even effect on the formation of aqueous biphasic systems formed by 1-alkyl-3-methylimidazolium chloride ionic liquids and salts. *J. Chem. Phys.* **2018**, *148*, 193842.
(42) Neves, C. M. S. S.; Freire, M. G.; Coutinho, J. A. P. Improved Recovery of Ionic Liquids from Contaminated Aqueous Streams Using Aluminium-Based Salts. *RSC Adv.* **2012**, *2*, 10882−10890.
(43) Bridges, N. J.; Gutowski, K. E.; Rogers, R. D. Investigation of Aqueous Biphasic Systems Formed from Solutions of Chaotropic Salts with Kosmotropic Salts (Salt−Salt ABS). *Green Chem.* **2007**, *9*, 177−183.
(44) Neves, C. M. S. S.; Silva, A. M. S.; Fernandes, A. M.; Coutinho, J. A. P.; Freire, M. G. Toward an Understanding of the Mechanisms behind the Formation of Liquid−Liquid Systems Formed by Two Ionic Liquids. *J. Phys. Chem. Lett.* **2017**, *8*, 3015−3019.
(45) *Chemspider—Search and share chemistry*; RSC, 2019. http://www.chemspider.com/.
(46) *Chemicalize—Instant Cheminformatic Solutions*; ChemAxon Ltd.; 2019. https://chemicalize.com/.
(47) Mashayekhi, F.; Meyer, A. S.; Shiigi, S. A.; Nguyen, V.; Kamei, D. T. Concentration of mammalian genomic DNA using two-phase aqueous micellar systems. *Biotechnol. Bioeng.* **2009**, *102*, 1613−1623.
(48) Xu, P.; Wang, Y.; Chen, J.; Wei, X.; Xu, W.; Ni, R.; Meng, J.; Zhou, Y. A novel aqueous biphasic system formed by deep eutectic solvent and ionic liquid for DNA partitioning. *Talanta* **2018**, *189*, 467−479.
(49) Huang, D. J.; Huang, D. C. The Research for the Extraction of Yeast's Nucleic Acid with [BMIM] BF4-H2O-KH2PO4 Ionic Liquid Aqueous Two-Phase System. *Adv. Mater. Res.* **2012**, 477−482.
(50) Ferreira, A. M.; Coutinho, J. A. P.; Fernandes, A. M.; Freire, M. G. Complete Removal of Textile Dyes from Aqueous Media Using Ionic-Liquid-Based Aqueous Two-Phase Systems. *Sep. Purif. Technol.* **2014**, *128*, 58−66.
(51) Cláudio, A. F. M.; Neves, M. C.; Shimizu, K.; Canongia Lopes, J. N.; Freire, M. G.; Coutinho, J. A. P. The Magic of Aqueous Solutions of Ionic Liquids: Ionic Liquids as a Powerful Class of Catanionic Hydrotropes. *Green Chem.* **2015**, *17*, 3948−3963.
(52) Cláudio, A. F. M.; Ferreira, A. M.; Freire, M. G.; Coutinho, J. A. P. Enhanced Extraction of Caffeine from Guaraná Seeds Using Aqueous Solutions of Ionic Liquids. *Green Chem.* **2013**, *15*, 2002−2010.
(53) Czarneckaa, J.; Cieslakb, M.; Michał, K. Application of solid phase extraction and high-performance liquid chromatography to

qualitative and quantitative analysis of nucleotides and nucleosides in human cerebrospinal fluid. *J. Chromatogr. B: Anal. Technol. Biomed. Life Sci.* **2005**, *822*, 85−90.

DOI: 10.1021/acs.jced.9b00452
J. Chem. Eng. Data XXXX, XXX, XXX−XXX